






# Characterisation of a common hotspot variant in acute intermittent porphyria sheds light on the mechanism of hydroxymethylbilane synthase function

Marthe S. Christie<sup>1,3</sup> , Mikko Laitaoja<sup>2</sup> , Aasne K. Aarsand<sup>3,4</sup> , Juha P. Kallio<sup>1</sup>  and Helene J. Bustad<sup>3</sup> 

<sup>1</sup> Department of Biomedicine, University of Bergen, Norway

<sup>2</sup> Department of Chemistry, University of Eastern Finland, Joensuu, Finland

<sup>3</sup> Norwegian Porphyria Centre (NAPOS), Department for Medical Biochemistry and Pharmacology, Haukeland University Hospital, Bergen, Norway

<sup>4</sup> Norwegian Organization for Quality Improvement of Laboratory Examinations, Haralds plass Deaconess Hospital, Bergen, Norway

## Keywords

acute intermittent porphyria; catalysis; haem; hydroxymethylbilane synthase; mass spectrometry; polypyrroles

## Correspondence

H. J. Bustad, Department for Medical Biochemistry and Pharmacology, Norwegian Porphyria Centre (NAPOS), Haukeland University Hospital, 5021 Bergen, Norway  
 E-mail: helene.bustad.johannessen@helsebergen.no

(Received 25 April 2022, revised 10 August 2022, accepted 16 September 2022)

doi:10.1002/2211-5463.13490

Edited by Cláudio Soares

[Correction added on 18 October 2022, after first online publication: Affiliation is corrected in PDF.]

Hydroxymethylbilane synthase (HMBS) is the third enzyme involved in haem biosynthesis, in which it catalyses the formation of tetrapyrrole 1-hydroxymethylbilane (HMB). In this process, HMBS binds four consecutive substrate molecules, creating the enzyme-intermediate complexes ES, ES<sub>2</sub>, ES<sub>3</sub> and ES<sub>4</sub>. Pathogenic variants in the *HMBS* gene are associated with the dominantly inherited disorder acute intermittent porphyria. In this study, we have characterised the p.R26H variant to shed light on the role of Arg26 in the elongation mechanism of HMBS and to provide insights into its effect on the enzyme. With selected biophysical methods, we have been able to show that p.R26H forms a single enzyme-intermediate complex in the ES<sub>2</sub>-state. We were also able to demonstrate that the p.R26H variant results in an inactive enzyme, which is unable to produce the HMB product.

Hydroxymethylbilane synthase (HMBS or porphobilinogen deaminase; PBGD) is the third enzyme in the haem biosynthetic pathway, where it catalyses the formation of the linear tetrapyrrole 1-hydroxymethylbilane (HMB) [1–3]. In this process, four consecutive PBG molecules are bound, creating the enzyme-intermediate complexes ES, ES<sub>2</sub>, ES<sub>3</sub>, and ES<sub>4</sub> respectively, as reviewed in Phillips [4]. Briefly, the elongation extends

from a dipyrromethane (DPM) cofactor, which is covalently bound to a cysteine in the active site [5,6]. DPM is formed by two PBG molecules and acts as a primer in the elongation process [7,8]. HMBS without bound cofactor (apo-HMBS) has, however, higher affinity for the HMB product than the substrate PBG, indicating that ES<sub>2</sub> may be formed directly from apo-HMBS [9].

## Abbreviations

AIP, acute intermittent porphyria; ALA, δ-aminolaevulinic acid; CD, circular dichroism; DPM, dipyrromethane; DSF, differential scanning fluorimetry; FT-ICR MS, Fourier transform ion cyclotron resonance mass spectrometry; HMB, 1-hydroxymethylbilane; HMBS, hydroxymethylbilane synthase; MD, molecular dynamics; PBG, porphobilinogen; SEC, size exclusion chromatography; TEV, tobacco etched virus.

In humans, there are two tissue-specific isoforms of HMBS derived from alternative splicing: the house-keeping (HMBS1) and the erythroid-specific (HMBS2) enzyme, with 361 and 344 amino acids, respectively. The 17 first amino acids at the N-terminus of HMBS1 have no known function, however, it has been suggested that they have a regulatory function or a role in e.g., protein trafficking [10,11].

Pathogenic variants in the *HMBS* gene are associated with the low penetrant autosomal dominant disorder acute intermittent porphyria (AIP). Both HMBS isoforms are affected if the variant is in the shared part of *HMBS* because of alternative splicing [12]. In *HMBS* gene variant carriers, wild-type (wt) enzyme expresses from one allele and the loss in total HMBS enzymatic activity can be up to 50%, depending on the variant [13]. However, many genetically predisposed carriers will never develop symptomatic disease, which is characterised by potentially life-threatening neurovisceral acute attacks, as the associated loss of HMBS activity is not sufficient for clinical expression, and the prevalence of likely pathogenic *HMBS* variants observed in the general population greatly outnumbers symptomatic disease prevalence [14]. In symptomatic AIP patients, clinical disease is associated with situations that increase the demand for haem, leading to an upregulation of  $\delta$ -aminolaevulinic acid (ALA) synthase 1, the first enzyme in the haem biosynthesis, whereupon the affected HMBS enzyme becomes rate-limiting [4]. In this setting, porphyrin precursors upstream from HMBS – ALA and porphobilinogen (PBG) – are produced in excess in the liver [15]. The overproduction and consequently accumulation of neurotoxic precursors are considered to be the cause of acute attacks. Increased levels of ALA and PBG in urine are used to diagnose AIP and other acute porphyrias in which ALA and PBG accumulate. AIP is associated with a varying natural history, from never-symptomatic carriers to patients with recurrent severe acute attacks. There is also a high phenotypic heterogeneity, even within the same family. Clinically, acute attacks are characterised by automatic dysfunction including severe abdominal pain, tachycardia, hypertension, and a wide range of neurological and psychiatric symptoms [15–17]. Acute attacks are triggered by various factors, most importantly drug-induced hepatic haem depletion via induction or suicidal inactivation of cytochrome P450 enzymes (CYPs) [18], hormonal changes associated with the menstrual cycle [19], low-calorie intake [20,21], infection and stress [22,23], though often a clear triggering factor cannot be established. Additionally, *HMBS* variant carriers are at risk of long-term complications including primary liver cancer, hypertension, and kidney failure [24–27]. Sporadic

acute attacks are treated by supportive measures and haem infusions, where the latter downregulates the hepatic ALAS1 activity through negative feedback. Currently, the only cure for AIP is liver transplantation [28], however, a recently introduced RNA interference therapy, Givosiran, has been shown to be effective in reducing attacks in patients with recurrent acute attacks [29,30].

More than 500 different *HMBS* variants associated with clinical disease, have been published [31]. However, for many variants, the effect on the HMBS enzyme has not been clearly described and the knowledge of the HMBS mechanism at the molecular level is still limited. Even with the numerous HMBS crystal structures and molecular dynamic (MD) simulations published in the last decades, the exact mechanisms of polypyrrole elongation are not yet completed through to the stage of Michaelis complex EP [32]. From the earliest studies, it was recognised that the enzyme in the crystal had to be with the cofactor in its active form [33].

Arg26 has been suggested to have a crucial role in the elongation process. Its location in hydrogen-bonding distance to the proposed substrate entry site (yellow, Fig. 1A), close to the available substrate and “growing end” of the intermediate complex where it can interact with the acetate of PBG, indicates a role in both positioning and possibly deaminating the incoming substrates [34,35]. The substitution of arginine 26 to histidine (Fig. 1B) results in a disease-associated variant (c.77G>A; p.R26H), which has been described in several different AIP families [36,37]. Two other missense substitutions at the same location, p.R26C and p.R26L, have also been reported [38–45]. In this work, we have sought to characterise the p.R26H variant to shed light on Arg26 and its role in the elongation mechanism of HMBS. Using a combination of anion-exchange chromatography, native PAGE, circular dichroism (CD), differential scanning fluorimetry (DSF), and high-resolution mass spectrometry, we demonstrate how the variant is trapped in the ES<sub>2</sub>-state, and that it is inactive without product turnover. Characterising HMBS variants in depth can provide an insight into their effect on the enzyme's structure and function, thereby providing more detailed information on the HMBS mechanism, allowing for a better understanding of genotype–phenotype correlations, and potentially providing useful information for future enzyme-specific treatment options.

## Materials and methods

Human wt-HMBS and variant were expressed in *Escherichia coli* BL21(DE3) strains as His-tagged fusion proteins

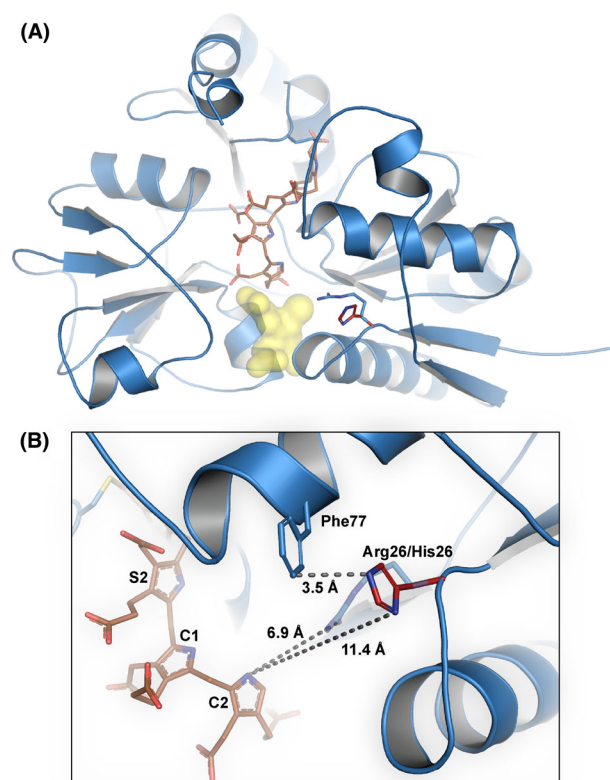


**Fig. 1.** Cartoon illustration of the hypothetical structure of p.R26H-HMBS in the ES<sub>2</sub> state. The figure is based on the structure of the p.R173W variant (PDB ID: 7AAK), prepared in the PYMOL MOLECULAR GRAPHICS SYSTEM, Version 2.5.2, Schrödinger, (LLC, New York, NY, USA). His26 has been modelled simply by substituting the Arg26 side chain using the most common side chain rotamer of histidine. The ES<sub>2</sub> substrate unit is in brown and His26 in dark red. The putative substrate entry site is shown in yellow, also representing the “growing end” on the C2 ring of the intermediate complex. (A) The overall structure of HMBS enzyme in the ES<sub>2</sub> state. (B) Close-up for Arg/His26 showing the distances to bound PBG and putative packing of His26 against Phe77.

with a tobacco etched virus (TEV) protease cleavage site (NLYFQ/G) in a pET-28a(+)-TEV vector. In this study, the erythroid-specific (HMBS2) enzyme was used but the numbering corresponding to the housekeeping isoform (HMBS1) was kept to match the reports from previous studies: p.R9H (c.26G>A) in the presented sequence equals to p.R26H (c.77G>A). HMBS expression constructs were purchased from GenScript Biotech (Piscataway, NJ, USA), with the following sequence for the variant:

(G) MRVIRVGT**HK**SQ**L**ARIQ**T**DSVVAT**L**KASY  
PGLQ**F**E**I**IAMST**T**GDK**I**LDT**A**LSK**I**GE**K**SL**F**  
TKE**L**EH**A**LE**K**NE**V**DL**V**VH**S**L**K**DL**P**TV**L**PP**G**F**T**  
I**G**A**I**CK**R**EN**P**H**D**AV**V**F**H**PK**F**V**G**KT**L**E**T**L**P**E**K**  
SV**V**GT**S**SL**R**RA**Q**L**Q**R**K**F**P**H**L**E**F**RS**I**R**G**N**L**N**T**  
RL**R**KL**D**E**Q**Q**E**F**S**A**I**IL**A**T**A**GL**Q**R**M**GW**H**NR**V**G

QILHPEECMYAVGQGALGVEVRAKDQDILDL  
VGVLHDPETLLRRCIAERAFLRHLEGGCSPVA  
VHTAMKDGQLYLTTGGVWSLDGSDSIQETMQA-  
TIHVPAQHEDGPEDDPQLVGITARNIPRGPQL  
AAQNLGISLANLLLSKGAKNILDVARQLNDAH

Theoretical masses: HMBS<sub>apo</sub>: 37 735.94 Da; ES<sub>2</sub>  
38573.22 Da; ES<sub>3</sub>: 38 782.29 Da.

### Protein expression and purification

Wt-HMBS and variant p.R26H were expressed in *E. coli* BL21 (DE3). Fifty millilitre Lennox LB EZmix™ (Merck KGaA, Darmstadt, Germany) starter cultures supplemented with 50 µg·mL<sup>-1</sup> kanamycin were grown overnight in a shaking incubator at 200 r.p.m. and 30 °C. The starter cultures were diluted in 1 L LB broth supplemented with kanamycin and incubated further at 200 r.p.m. and 37 °C until OD<sub>600</sub> of 0.5–0.6 before induction with 0.5 mM IPTG and further incubated overnight at 200 r.p.m. and 27 °C. Cells were harvested at 6000 g for 30 min and pellets were resuspended in 15 mL wash buffer: 400 mM NaCl, 25 mM Tris at pH 8, 20 mM imidazole at pH 7.5, 0.5 mM tris (2-carboxyethyl) phosphine (TCEP) added protease inhibitors (1 tablet cOmplete™ w/EDTA (Roche Diagnostics GmbH, Mannheim, Germany), 10 mM benzamide and 0.2 mM PMSF). Resuspended pellets were frozen at –20 °C until use.

The resuspended pellet was thawed on ice and lysis buffer was added to 40 mL before sonication on ice for 3 × 2 min at 25 W output with 10 s pulses and pauses on ice, then centrifuged at 20 000 g for 45 min. The supernatant was loaded onto a nickel-charged affinity resin (Ni-NTA Agarose; Qiagen, Hilden, Germany) equilibrated in wash buffer, using a gravity flow purification column for His-tag affinity chromatography. The resin was washed 3 × CV with wash buffer before eluting the protein with 400 mM NaCl, 25 mM Tris at pH 8, 400 mM imidazole at pH 7.5 and 0.5 mM TCEP.

Eluted His-tagged HMBS was added 1 : 100 TEV protease to cleave off the fusion tag, during dialysis with 400 mM NaCl, 25 mM Tris pH 8 and 0.5 mM TCEP in a cellulose membrane dialysis tubing with MW cut-off at 14 000 ON at 4 °C. Cleaved protein was run through Ni-NTA pre-equilibrated with 150 mM NaCl, 25 mM Tris pH 8 and 0.5 mM TCEP, collected and concentrated using Amicon Ultra centrifugal 30 kDa cut-off filters (Merck) at 4000 g. NanoDrop spectrophotometer (Thermo Fisher Scientific Inc., Waltham, MA, USA) and sequence-derived extinction coefficients were used to determine protein concentrations.

Concentrated wt-HMBS and p.R26H were further purified by size exclusion chromatography (SEC) on a GE HiLoad Superdex 75 16/60 PG column connected to an Äkta Pure Protein Purification System (Cytiva Europe GmbH, Freiburg, Germany) at 4 °C, using 30 mM NaCl, 25 mM Tris pH 8 (buffer A) at flow rate 1 mL·min<sup>-1</sup>.

## Anion-exchange chromatography

Anion-exchange chromatography using a Mono Q 4.6/100 column (Cytiva) connected to an Äkta Pure (Cytiva) was used to separate the enzyme-intermediate complexes. The Mono Q column was equilibrated in buffer A at 4 °C. The protein was eluted in a gradient from 0% to 65% using 400 mM NaCl, 25 mM Tris pH 8 (buffer B) at 4 °C and peak fractions were collected. The isolated intermediates were concentrated using Amicon Ultra centrifugal 30 kDa cut-off filters (Merck) for further analyses.

## Polyacrylamide gel electrophoresis

Proteins were analysed by native polyacrylamide gel electrophoresis (native-PAGE) with a loading buffer of 125 mM Tris-HCl, 40% glycerol, 0.002% bromophenol blue. The samples were loaded on a 10% Mini-PROTEAN<sup>®</sup> TGX<sup>™</sup> Precast Protein Gel (Bio-Rad Laboratories, Hercules, CA, USA) and ran for 2½ h at 140 V and 4 °C. The gel was stained with Coomassie blue staining and visualised by Molecular Imager ChemiDoc XRS+ with IMAGELAB software (Bio-Rad).

## Circular dichroism spectroscopy

Far-UV spectra were obtained using a J-810 Jasco spectropolarimeter (Jasco Europe S.R.L., Cremella, Italia) with a CDF-426S Peltier element (Jasco) for temperature control and a 300 µL quartz cuvette with a path length of 1 mm. Wt-HMBS and p.R26H at 5 µM were prepared in 10 mM K<sub>2</sub>HPO<sub>4</sub>, 100 mM NaF. Three scans were obtained for each spectrum and the buffer scans were subtracted using the integrated Spectra Manager<sup>™</sup> software. DichroWeb and the CDSSTR analysis method with reference set 3, were used for secondary structure predictions [46,47].

## Enzymatic activity

The enzymatic activity was assayed by adding 2 µg enzyme to 50 mM Tris-HCl at pH 8 and pre-incubating the sample for 3 min at 37 °C. To start the enzyme reaction 100 µM prewarmed PBG was added, and the reaction was stopped by adding 5 M HCl and 0.1% benzoquinone after 4 min. Benzoquinone oxidised the produced uroporphyrinogen I into uroporphyrin in the dark on ice for 30 min. The sample was subsequently centrifuged to remove precipitated protein, before the absorbance of uroporphyrin was measured at 405 nm ( $\epsilon = 548\,000\text{ M}^{-1}\cdot\text{cm}^{-1}$ ) using a Nano-Drop spectrophotometer. HMBS activity was expressed as nmol uroporphyrinogen I per hour per mg under the given conditions. Michaelis-Menten kinetics was used to determine the kinetic parameters;  $K_m$  and  $V_{max}$  were obtained using a range of PBG concentrations from 3.125–2000 µM and analysed using the Michaelis-Menten enzyme kinetics

model in GRAPHPAD PRISM (GraphPad Prism version 9.2.0 for MacOS; GraphPad Software, San Diego, CA, USA, [www.graphpad.com](http://www.graphpad.com)).

## Mass spectrometry

Prior to mass spectrometric experiments, the enzyme samples were buffer-exchanged to 20 mM NH<sub>4</sub>OAc pH 6.8 using PD Miditrap G-25 column (Cytiva). Their concentrations were determined by UV absorbance at  $A_{280}$  using their sequence-derived extinction coefficient ( $15\,470\text{ M}^{-1}\cdot\text{cm}^{-1}$ ). Further dilutions were made using HPLC quality acetonitrile, water, and acetic acid. Mass spectra were measured using a Bruker 12-T solariX XR FT-ICR mass spectrometer (Bruker Daltonik GmbH, Bremen, Germany). The substrate reactions were undertaken using Bruker timsTOF mass spectrometer (Bruker Daltonik). All samples were measured by direct infusion, at  $2\text{ }\mu\text{L}\cdot\text{min}^{-1}$ , using standard electrospray source. The instrument was calibrated using NaPFHA clusters before measurements. The mass spectrometer was operated using FTMSCONTROL 2.2 software, and the data were processed using the BRUKER DATAANALYSIS 5.1 software. Deconvolution (i.e., zero-charge) spectra were calculated using a Maximum Entropy (MAXENT) deconvolution algorithm, built into the software. All masses are reported as most abundant isotopic masses.

## Differential scanning fluorimetry

A Light Cycler 480 Real-Time PCR (Roche) was used to obtain thermal denaturing scans. Five micromolar protein was prepared in phosphate-buffered saline with 5× SYPRO Orange (Agilent Technologies, Santa Clara, CA, USA) and analysed in 384-well plates, as previously described [48]. Unfolding curves were recorded at a scan rate of  $2\text{ }^\circ\text{C}\cdot\text{min}^{-1}$  with 0.2 °C intervals from 20 °C to 99 °C. Data were analysed using HTSDSF EXPLORER [49].

## Results

In this work, we have utilised the recombinant HMBS wt and variant p.R9H, both in the human HMBS2 isoform (NM\_001024382.2:c.26G>A), which corresponds to p.R26H in the HMBS1 isoform (NM\_000190.4:c.77G>A). There are minimal structural and no known functional differences between these two isoforms [11]. To keep consistency with the literature, we will refer to the constructs in this work as wt-HMBS and the variant as p.R26H.

The recombinant p.R26H was successfully purified, in amounts similar to the wt-HMBS. CD spectroscopy was performed prior to further experiments to confirm secondary structural composition and fold. A comparison of wt-HMBS and p.R26H (Fig. 2A) clearly

indicated the correct folding of the variant, which was further clarified by the estimation of the secondary structural content (Table S1).

Purified HMBS can be further separated into its enzyme intermediates' complexes, using anion-exchange chromatography with a buffer gradient [11,48,50]. Comparing results for wt-HMBS and p.R26H, it was evident that p.R26H mainly eluted as a single intermediate at ~26% of gradient buffer B (Fig. 2B), corresponding to ES<sub>2</sub> in wt-HMBS. Native PAGE has commonly been used to demonstrate the enzyme-intermediate complexes, because of the difference in net charge between them [11,48,51]. As seen in Fig. 2B, lane 1, all the expected bands from wt-HMBS were observed. On the other hand, p.R26H migrated as one major band

(Fig. 2B, lane 2), with minor bands corresponding to the smaller peaks in the chromatogram (Fig. 2B). The isolated main peak of p.R26H is shown in Fig. 2B, lane 3. The migration pattern of p.R26H was inconclusive, as the major peak migrated further than the ES<sub>2</sub> of wt-HMBS. Using Fourier transform ion cyclotron resonance mass spectrometry (FT-ICR MS), the intermediate complex distribution in both wt- and variant HMBS was analysed, as previously reported [52]. FT-ICR MS measurements in denaturing conditions verified the findings for p.R26H, being mainly present in the intermediate ES<sub>2</sub>-state (Fig. 2C). The tailing of the ES<sub>2</sub> peak was most likely caused by incomplete desalting. Uroporphyrinogen was also observed (Fig. S1A), indicating that this cyclic product has affinity for and can be

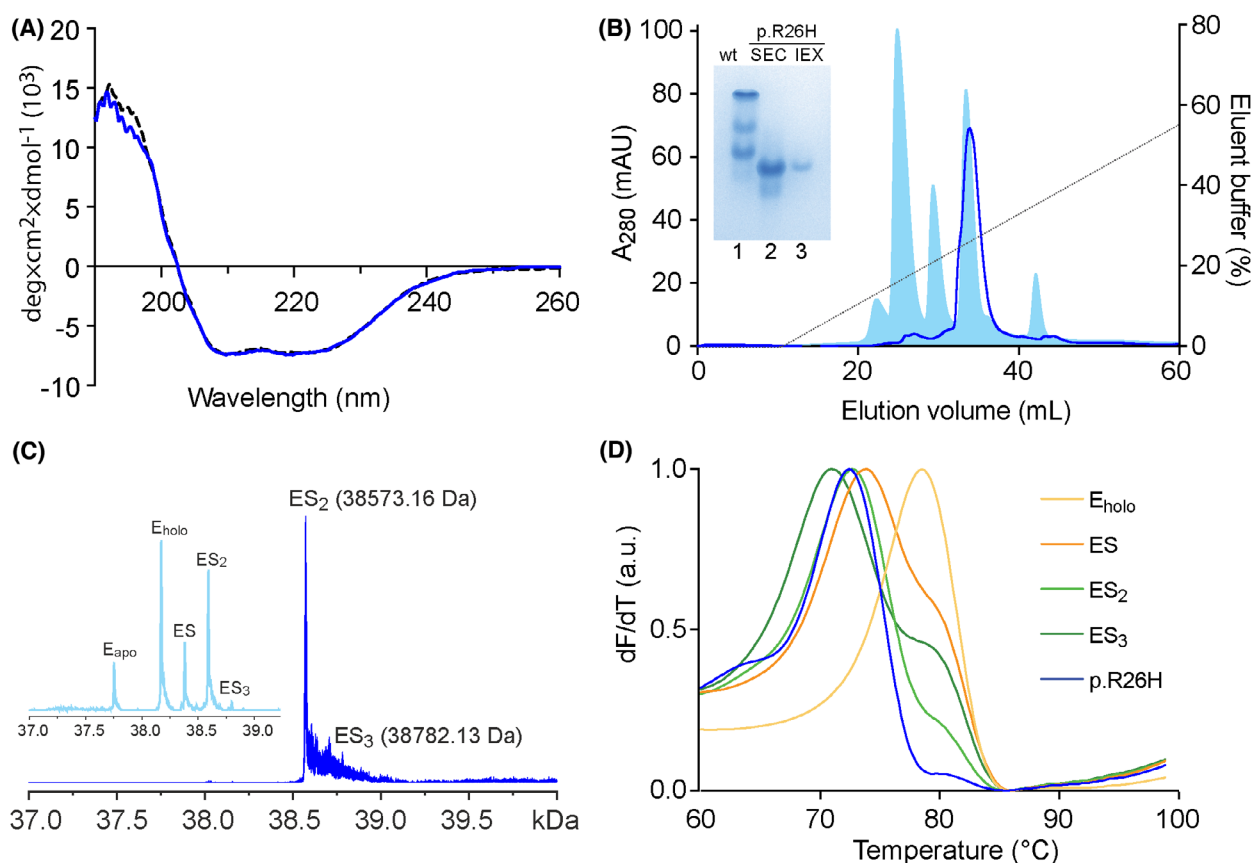


**Fig. 2.** Biophysical characterisation of HMBS variant p.R26H. Purification and detection of enzyme-intermediate complexes of wt- and p.R26H HMBS. (A) Far-UV CD spectroscopy of HMBS. 0.2 mg·mL<sup>-1</sup> wt-HMBS (grey solid line) and p.R26H variant (blue line) analysed in triplicates, corrected for concentration. (B) Isolation of enzyme-intermediate complexes. Recombinantly expressed wt-HMBS (light blue) and p.R26H (blue) enzyme-intermediate complexes are separated and isolated using anion-exchange chromatography. Inset: Native-PAGE analysis of wt-HMBS (lane 1), p.R26H from SEC (lane 2), and the isolated main peak of p.R26H intermediate from anion-exchange chromatography (IEX, lane 3). (C) Charge-deconvoluted ESI FT-ICR spectrum of p.R26H. The p.R26H variant was measured in denaturing conditions at 1 μM protein concentration. The variant was detected mainly as ES<sub>2</sub> (38 573.16 Da) and there was small amounts of ES<sub>3</sub> (38 782.13 Da). Inset: Purified wt-HMBS enzyme showing a mixture of intermediates (E<sub>apo</sub>, E<sub>holo</sub>, ES, ES<sub>2</sub> and ES<sub>3</sub>). (D) Thermal denaturation of p.R26H monitored by DSF. The first derivative of unfolding as a function of temperature is shown as the average of four in-plate replicates. The intermediates from wt-HMBS are E<sub>holo</sub> (yellow), ES (orange), ES<sub>2</sub> (light green), and ES<sub>3</sub> (dark green). The p.R26H variant is shown in blue.

co-purified with the enzyme [9]. Uroporphyrinogen I or III can be derived from either recombinant HMBS or endogenous *E. coli* HMBS enzyme activity, respectively. The native-like conditions confirmed that the Arg-to-His substitution did not cause any unfolding of the enzyme (Fig. S1B). As expected, intermediates corresponding with  $E_{\text{holo}}$ , ES, ES<sub>2</sub> and ES<sub>3</sub> were detected in wt-HMBS (Fig. 2C, inset and Fig. S2A).

Wt-HMBS demonstrated a specific activity of  $2249 \pm 38 \text{ nmol}\cdot\text{mg}^{-1}\cdot\text{h}^{-1}$ , however, p.R26H was completely inactive and incapable of producing the HMB product. Hence, the kinetic parameters of the variant could not be determined, whereas we obtained a  $V_{\text{max}}$  of  $2996 \pm 9 \text{ nmol}\cdot\text{mg}^{-1}\cdot\text{h}^{-1}$  and  $K_{\text{m}}$  of  $28 \pm 1 \mu\text{M}$  for wt-HMBS (Fig. S3). FT-ICR MS showed a rapid formation ( $\sim 1 \text{ min}$ ) of the ES<sub>4</sub> intermediate when wt-HMBS was incubated with  $10\times$  PBG (Fig. S2B), and after 60 min the intermediate distribution reappeared, indicating depletion of the substrate (Fig. S2C). The addition of  $10\times$  PBG to p.R26H and incubation up to 24 h did not change the distribution (Fig. S2D), further corroborating that the p.R26H is inactive without the capacity of turnover.

We have previously demonstrated that the thermostability of HMBS decreases with the number of bound PBG substrates [48]. We wanted to investigate whether the Arg-to-His substitution had an impact on the structural stability, or if the effect could be attributed solely to the change in amino acid. Therefore, we analysed the thermostability of the isolated wt and variant enzyme-intermediate complexes, using DSF. The wt-HMBS intermediates demonstrated a loss in the half-denaturing temperature ( $T_{\text{m}}$ ) represented as maxima of the first derivative ( $dF/dT$ ) from  $78.6 \pm 0.1 \text{ }^{\circ}\text{C}$  to  $71.0 \pm 0.2 \text{ }^{\circ}\text{C}$  for  $E_{\text{holo}}$  and ES<sub>3</sub>, respectively (Fig. 2D). The  $T_{\text{m}}$ -value of the isolated intermediate in p.R26H variant was  $72.6 \pm 0.1 \text{ }^{\circ}\text{C}$ , corresponding to the ES<sub>2</sub> of wt-HMBS, which was  $72.8 \pm 0.1 \text{ }^{\circ}\text{C}$ .

## Discussion

Arg26 is one of many conserved arginine residues across species and has been implicated to be critical for HMBS catalysis [53,54]. In crystal structures PDB IDs 1PDA and 3ECR, Arg26 has been observed in hydrogen-bonding distance to an acetate or sulphate ion (derived from solutions used in the crystallisation process) located in the predicted substrate-binding site [34,55]. Other crystal structures such as PDB IDs 5M6R and 7AAK also indicate several intradomain interactions for Arg26, such as Pi-cation interaction with Phe77, hydrophobic alkyl interaction with Ala31

and Leu81, hydrogen-bond to Thr25 and electrostatic interactions with Asp99 [11,52], indicating its important location in the active site, and putative role in both enzyme activity and structural stability. Sato et al. [50] demonstrated that Arg26, Arg167 and Arg173 all interact with the substrate analogue positioned in the substrate-binding site. Interestingly, previously described variants p.R167W and p.R173W, both interacting with the propionate side chain of PBG, exhibit different effects, where the first can form all enzyme-intermediate complexes, whereas the latter creates a catalytic blockage and a subsequent accumulation of a single intermediate [52]. Our results demonstrate that p.R26H also results in a variant that is catalytically blocked with ES<sub>2</sub> as the accumulated intermediate, however, no major structural changes are indicated based on secondary structure content and thermostability analysis.

Arg26 in humans corresponds to Arg11 in *E. coli* HMBS. The p.R11H and p.R11L variants expressed in *E. coli* were reported as correctly folded but unable to bind substrate [54,56]. Interestingly, two previous reports on the human p.R26H variant have incongruent observations, with one suggesting altered interaction with the cofactor and the other no pyrrole chain elongation [43,57]. However, we do not have direct evidence of the formation of ES<sub>2</sub> from ES, and cannot rule out that endogenous HMBS produces HMB product that interacts directly with apo-variant resulting in the ES<sub>2</sub> complex without involving Arg26 proton donation, as has also been suggested for variants of D84 in *E. coli* [9].

Recent advances in the field include the crystal structure of wt-HMBS in its ES<sub>2</sub>-state (PDB ID: 5M6R), demonstrating how the cofactor-binding loop with the Cys261 residue that anchors the cofactor, is pulled backwards with the two incoming PBG substrates [11]. The two new substrate molecules replace the cofactor in their positions and interactions [11,52]. Furthermore, our report on the p.R173W-variant trapped in the ES<sub>2</sub>-state (PDB ID: 7AAK) revealed that Arg173 is an essential residue for the enzyme to move from ES<sub>2</sub> to ES<sub>3</sub> in the elongation process [52]. Despite providing new structural information, neither of these reports, naturally, could offer any light on details beyond the ES<sub>2</sub>-state, or the role of Arg26 in the elongation process. Nevertheless, the critical function of Arg26 in enzymatic catalysis has been described based on docking and MD simulations, which suggested Arg26 as the most likely proton donor in the forming of ES and ES<sub>2</sub>, but too far away for the next step from ES<sub>2</sub> to ES<sub>3</sub> and beyond [53]. However, it was assumed that the elongation process extended from the cofactor without involving a

rearrangement of the cofactor-binding loop [53], a movement that has later been demonstrated in other reports [11,52]. Our current results support that Arg26 is essential for the formation of the intermediates up to the ES<sub>2</sub> state, possibly in concert with Arg173, where Arg173 likely acts as the coordinator for the bound PBG also stabilising the structure, and where Arg26 has the role as proton donor for upcoming substrates. Both p.R173W and p.R26H are trapped in the ES<sub>2</sub>-state, however, neither have, in our studies, responded to the addition of excess substrate. Where p.R173W displays some structural instability as a function of temperature [48], p.R26H resembles wt-HMBS in the ES<sub>2</sub>-state in its reaction to temperature. This could be explained by the direct interaction between Arg173 and the bound PBG, where the Arg → Trp substitution disturbs the stabilising hydrogen-bond network, which connects the structural domains via the bound PBG, and yields a lowered thermostability, whereas the interactions that are lost when Arg26 is replaced by His has little or no impact on the structural stability. In addition, the similar secondary structure content between wt-HMBS and p.R26H indicates that the overall secondary structure is not affected by the introduction of the histidine. Modelling of the variant based on existing high-resolution ES<sub>2</sub>-structure (PDB ID: 7AAK) was therefore seen as sufficient to illustrate the p.R26H structure (Fig. 1).

Bung et al. [53] also predict, via MD simulations, that Arg26 interacts with both Thr58 and Asp61. Asp61 is located in the active-site loop and is a highly conserved residue, predicted to have important interactions contributing to the stability of the structure [58]. Interestingly, Arg173 is also in the vicinity of Asp61 considering the flexible nature of the active-site loop, and it could be speculated that these three residues act in concert. Based on structural evidence, the interactions between Arg26 and the active-site loop (residues Ser57-Lys74) can only occur when the is loop completely closed as shown in the HMBS structure from *Arabidopsis thaliana* (PDB ID: 4HTG) [59]. In this structure, the cofactor is in its oxidised form. Thus, we cannot conclude that the closing of the active-site loop occurs as a part of the elongation process. However, p.D61N, p.D61H, and p.D61Y are known pathogenic variants of Asp61 [60–62] indicating the importance of the loop and these residues for the function of the enzyme.

The p.R26H variant has been reported in several different families with AIP, originating in different countries and spanning several continents. In AIP, there is a large molecular heterogeneity and most variants are restricted to single or just a few families, but the p.R26H occurs at a known hotspot involving CpG dinucleotides [63] and

has also been described to occur *de novo* [36,37]. Most publications on p.R26H have diagnostic data, but there is relatively little clinical data included and thus any assessment of severity such as early symptom onset or clinical penetrance is therefore not possible. However, generally, few genotype–phenotype correlations have yet been established in AIP and only null-allele variants have been described to be associated with a more severe phenotype and higher penetrance [57].

Overall, characterising a pathogenic variant alone does not explain a correlation between genotype and phenotype, and the clinical penetrance of *HMBS* variants is most likely modulated by other genetic and environmental factors [57]. Nevertheless, our report, together with previous variant characterisation at the protein level, demonstrates how the effect of missense substitutions can be grouped into at least two groups where (a) the enzyme has residual activity yielding some turnover of protein, and (b) the enzyme is blocked for turnover in a single intermediate state. These findings can be important in future work exploring alternative treatment options for patients suffering from AIP.

## Acknowledgements

We thank Prof Aurora Martinez and Prof Janne Jänis for lab facilities, discussions, and collaboration. This work was supported by grants from the Western Norway Regional Health Authority (project F-12142 and F-11928 to AKA), the Norwegian National Advisory Unit on Rare Disorders (to AKA, MCS and HJB), Helse Bergen Haukeland University Hospital Health Trust (project F11737-D11022 to AKA) and by the Norwegian Research Council (grant BIOTEK2021 285295 to JPK). The FT-ICR facility is supported by the European Regional Development Fund (Grant A70135), Biocenter Kuopio, Instruct-FI (Biocenter Finland) and the EU Horizon 2020 Research and Innovation Programme- (European Network of Fourier Transform Ion Cyclotron Resonance Mass Spectrometry Centers, EU FT-ICR MS; Grant Agreement 731077). We are grateful to Prof John R. Helliwell for pre-reviewing the manuscript. We acknowledge the use of the Core Facility for Biophysics, Structural Biology and Screening (BiSS) at the University of Bergen, which has received infrastructure funding from the Research Council of Norway through NOR-CRYST (grant number 245828 and NOR-Openscreen (grant number 245922)). One of the authors of this publication is a member of the European Reference Network for Rare Hereditary Metabolic Disorders (MetabERN) – Project ID No. 739543.

## Conflict of interest

The authors declare no conflict of interest.

## Data accessibility

The data that support the findings of this study are available from the corresponding author helene.bustad.johannessen@helse-bergen.no upon reasonable request.

## Author contributions

AKA, JPK and HJB conceived the study; JPK and HJB designed experiments and supervised the study; MSC and ML performed experiments; MSC, ML, JPK and HJB analysed data; MSC wrote the first manuscript draft; AKA, JPK and HJB made revisions and finalised the manuscript.

## References

- Battersby AR, Fookes CJR, Gustafson-Potter KE, Matcham GWJ, McDonald E. Proof by synthesis that unrearranged hydroxymethylbilane is the product from deaminase and the substrate for cosynthetase in the biosynthesis of uro<sup>3</sup>gen-III. *J Chem Soc Chem Commun.* 1979;1155–8. <https://doi.org/10.1039/C39790001155>
- Burton G, Fagerness PE, Hosozawa S, Jordan PM, Scott AI. <sup>13</sup>C n.m.r. evidence for a new intermediate, pre-uroporphyrinogen, in the enzymic transformation of porphobilinogen into uroporphyrinogens I and III. *J Chem Soc Chem Commun.* 1979;202–4. <https://doi.org/10.1039/C39790000202>
- Scott AI, Burton G, Jordan PM, Matsumoto H, Fagerness PE, Pryde LM. N.m.r. spectroscopy as a probe for the study of enzyme-catalysed reactions. Further observations of preuoporphyrinogen, a substrate for uroporphyrinogen III cosynthetase. *J Chem Soc Chem Commun.* 1980;384–7. <https://doi.org/10.1039/C39800000384>
- Phillips JD. Heme biosynthesis and the porphyrias. *Mol Genet Metab.* 2019;128:164–77.
- Miller AD, Hart GJ, Packman LC, Battersby AR. Evidence that the pyrromethane cofactor of hydroxymethylbilane synthase (porphobilinogen deaminase) is bound to the protein through the sulphur atom of cysteine-242. *Biochem J.* 1988;254:915–8.
- Jordan PM, Warren MJ, Williams HJ, Stolowich NJ, Roessner CA, Grant SK, et al. Identification of a cysteine residue as the binding site for the dipyrromethane cofactor at the active site of *Escherichia coli* porphobilinogen deaminase. *FEBS Lett.* 1988;235:189–93.
- Hart GJ, Miller AD, Leeper FJ, Battersby AR. Biosynthesis of the natural porphyrins: proof that hydroxymethylbilane synthase (porphobilinogen deaminase) uses a novel binding group in its catalytic action. *J Chem Soc Chem Commun.* 1987;1762–5. <https://doi.org/10.1039/C39870001762>
- Jordan PM, Warren MJ. Evidence for a dipyrromethane cofactor at the catalytic site of *E. coli* porphobilinogen deaminase. *FEBS Lett.* 1987;225:87–92.
- Shoolingin-Jordan PM, Warren MJ, Awan SJ. Discovery that the assembly of the dipyrromethane cofactor of porphobilinogen deaminase holoenzyme proceeds initially by the reaction of preuroporphyrinogen with the apoenzyme. *Biochem J.* 1996;316(Pt 2):373–6.
- Brons-Poulsen J, Christiansen L, Petersen NE, Horder M, Kristiansen K. Characterization of two isoalleles and three mutations in both isoforms of purified recombinant human porphobilinogen deaminase. *Scand J Clin Lab Invest.* 2005;65:93–105.
- Pluta P, Roversi P, Bernardo-Seisdedos G, Rojas AL, Cooper JB, Gu S, et al. Structural basis of pyrrole polymerization in human porphobilinogen deaminase. *Biochim Biophys Acta Gen Subj.* 2018;1862:1948–55.
- Grandchamp B, De Verneuil H, Beaumont C, Chretien S, Walter O, Nordmann Y. Tissue-specific expression of porphobilinogen deaminase. Two isoenzymes from a single gene. *Eur J Biochem.* 1987;162:105–10.
- Badminton MN, Elder GH. Molecular mechanisms of dominant expression in porphyria. *J Inherit Metab Dis.* 2005;28:277–86.
- Chen B, Solis-Villa C, Hakenberg J, Qiao W, Srinivasan RR, Yasuda M, et al. Acute intermittent porphyria: predicted pathogenicity of HMBS variants indicates extremely low penetrance of the autosomal dominant disease. *Hum Mutat.* 2016;37:1215–22.
- Bissell DM, Anderson KE, Bonkovsky HL. Porphyria. *N Engl J Med.* 2017;377:862–72.
- Bonkovsky HL, Dixon N, Rudnick S. Pathogenesis and clinical features of the acute hepatic porphyrias (AHPs). *Mol Genet Metab.* 2019;128:213–8.
- Stein PE, Badminton MN, Rees DC. Update review of the acute porphyrias. *Br J Haematol.* 2017;176:527–38.
- Correia MA, Sinclair PR, De Matteis F. Cytochrome P450 regulation: the interplay between its heme and apoprotein moieties in synthesis, assembly, repair, and disposal. *Drug Metab Rev.* 2011;43:1–26.
- Innala E, Backstrom T, Bixo M, Andersson C. Evaluation of gonadotropin-releasing hormone agonist treatment for prevention of menstrual-related attacks in acute porphyria. *Acta Obstet Gynecol Scand.* 2010;89:95–100.
- Delaby C, To-Figueras J, Deybach JC, Casamitjana R, Puy H, Herrero C. Role of two nutritional hepatic



- markers (insulin-like growth factor 1 and transthyretin) in the clinical assessment and follow-up of acute intermittent porphyria patients. *J Intern Med.* 2009;**266**:277–85.
- 21 Handschin C, Lin J, Rhee J, Peyer AK, Chin S, Wu PH, et al. Nutritional regulation of hepatic heme biosynthesis and porphyria through PGC-1 $\alpha$ . *Cell.* 2005;**122**:505–15.
  - 22 Bylesjo I, Wikberg A, Andersson C. Clinical aspects of acute intermittent porphyria in northern Sweden: a population-based study. *Scand J Clin Lab Invest.* 2009;**69**:612–8.
  - 23 Eales L. Porphyria and the dangerous life-threatening drugs. *S Afr Med J.* 1979;**56**:914–7.
  - 24 Pallet N, Mami I, Schmitt C, Karim Z, Francois A, Rabant M, et al. High prevalence of and potential mechanisms for chronic kidney disease in patients with acute intermittent porphyria. *Kidney Int.* 2015;**88**:386–95.
  - 25 Baravelli CM, Sandberg S, Aarsand AK, Nilsen RM, Tollanes MC. Acute hepatic porphyria and cancer risk: a nationwide cohort study. *J Intern Med.* 2017;**282**:229–40.
  - 26 Saberi B, Naik H, Overbey JR, Erwin AL, Anderson KE, Bissell DM, et al. Hepatocellular carcinoma in acute hepatic porphyrias: results from the longitudinal study of the U.S. Porphyrias Consortium. *Hepatology.* 2021;**73**:1736–46.
  - 27 Lissing M, Vassiliou D, Floderus Y, Harper P, Bottai M, Kotopouli M, et al. Risk of primary liver cancer in acute hepatic porphyria patients: a matched cohort study of 1,244 individuals. *J Intern Med.* 2022;**291**(6):824–36.
  - 28 Lissing M, Nowak G, Adam R, Karam V, Boyd A, Gouya L, et al. Liver transplantation for acute intermittent porphyria. *Liver Transpl.* 2021;**27**:491–501.
  - 29 Balwani M, Sardh E, Gouya L. Givosiran for acute intermittent porphyria. Reply. *N Engl J Med.* 2020;**383**:1989–90.
  - 30 Poli A, Schmitt C, Moulouel B, Mirmiran A, Talbi N, Riviere S, et al. Givosiran in acute intermittent porphyria: a personalized medicine approach. *Mol Genet Metab.* 2022;**135**(3):206–14.
  - 31 Bustad HJ, Kallio JP, Vorland M, Fiorentino V, Sandberg S, Schmitt C, et al. Acute intermittent porphyria: an overview of therapy developments and future perspectives focusing on stabilisation of HMBS and proteostasis regulators. *Int J Mol Sci.* 2021;**22**:675.
  - 32 Helliwell JR. The crystal structures of the enzyme hydroxymethylbilane synthase, also known as porphobilinogen deaminase. *Acta Crystallogr F Struct Biol Commun.* 2021;**77**:388–98.
  - 33 Hadener A, Matzinger PK, Battersby AR, McSweeney S, Thompson AW, Hammersley AP, et al. Determination of the structure of seleno-methionine-labelled hydroxymethylbilane synthase in its active form by multi-wavelength anomalous dispersion. *Acta Crystallogr D Biol Crystallogr.* 1999;**55**:631–43.
  - 34 Louie GV, Brownlie PD, Lambert R, Cooper JB, Blundell TL, Wood SP, et al. Structure of porphobilinogen deaminase reveals a flexible multidomain polymerase with a single catalytic site. *Nature.* 1992;**359**:33–9.
  - 35 Song G, Li Y, Cheng C, Zhao Y, Gao A, Zhang R, et al. Structural insight into acute intermittent porphyria. *FASEB J.* 2009;**23**:396–404.
  - 36 Younger DS, Tanji K. Demyelinating neuropathy in genetically confirmed acute intermittent porphyria. *Muscle Nerve.* 2015;**52**:916–7.
  - 37 Puy H, Deybach JC, Lamoril J, Robreau AM, Da Silva V, Gouya L, et al. Molecular epidemiology and diagnosis of PBG deaminase gene defects in acute intermittent porphyria. *Am J Hum Genet.* 1997;**60**:1373–83.
  - 38 Goncharova M, Pshenichnikova O, Luchinina Y, Pustovoyt Y, Karpova I, Surin V. Molecular genetic study of acute intermittent porphyria in Russia: HMBS gene mutation spectrum and problem of penetrance. *Clin Genet.* 2019;**96**:91–7.
  - 39 To-Figueras J, Badenas C, Carrera C, Munoz C, Mila M, Lecha M, et al. Genetic and biochemical characterization of 16 acute intermittent porphyria cases with a high prevalence of the R173W mutation. *J Inherit Metab Dis.* 2006;**29**:580–5.
  - 40 Kauppinen R, Mustajoki S, Pihlaja H, Peltonen L, Mustajoki P. Acute intermittent porphyria in Finland: 19 mutations in the porphobilinogen deaminase gene. *Hum Mol Genet.* 1995;**4**:215–22.
  - 41 Moran-Jimenez MJ, Borrero-Corte MJ, Jara-Rubio F, Garcia-Pastor I, Diaz-Diaz S, Castelbon-Fernandez FJ, et al. Molecular analysis of 55 Spanish patients with acute intermittent porphyria. *Genes (Basel).* 2020;**11**:924.
  - 42 Mendez M, Moran-Jimenez MJ, Gomez-Abecia S, Garcia-Bravo M, Garrido-Astray MC, Fontanellas A, et al. Identification and characterization of HMBS gene mutations in Spanish patients with acute intermittent porphyria. *Cell Mol Biol (Noisy-le-Grand).* 2009;**55**:55–63.
  - 43 Ulbrichova D, Hrdinka M, Saudek V, Martasek P. Acute intermittent porphyria—impact of mutations found in the hydroxymethylbilane synthase gene on biochemical and enzymatic protein properties. *FEBS J.* 2009;**276**:2106–15.
  - 44 Floderus Y, Shoolingin-Jordan PM, Harper P. Acute intermittent porphyria in Sweden. Molecular, functional and clinical consequences of some new mutations found in the porphobilinogen deaminase gene. *Clin Genet.* 2002;**62**:288–97.
  - 45 Yang CC, Kuo HC, You HL, Wang J, Huang CC, Liu CY, et al. HMBS mutations in Chinese patients with

- acute intermittent porphyria. *Ann Hum Genet.* 2008;**72**:683–6.
- 46 Miles AJ, Ramalli SG, Wallace BA. DichroWeb, a website for calculating protein secondary structure from circular dichroism spectroscopic data. *Protein Sci.* 2022;**31**:37–46.
- 47 Sreerama N, Woody RW. Estimation of protein secondary structure from circular dichroism spectra: comparison of CONTIN, SELCON, and CDSSTR methods with an expanded reference set. *Anal Biochem.* 2000;**287**:252–60.
- 48 Bustad HJ, Vorland M, Ronneseth E, Sandberg S, Martinez A, Toska K. Conformational stability and activity analysis of two hydroxymethylbilane synthase mutants, K132N and V215E, with different phenotypic association with acute intermittent porphyria. *Biosci Rep.* 2013;**33**:e00056.
- 49 Martin-Malpartida P, Hausvik E, Underhaug J, Torner C, Martinez A, Macias MJ. HTSDSF Explorer, a novel tool to analyze high-throughput dsf screenings. *J Mol Biol.* 2021;**434**(11):167372.
- 50 Sato H, Sugishima M, Tsukaguchi M, Masuko T, Iijima M, Takano M, et al. Crystal structures of hydroxymethylbilane synthase complexed with a substrate analog: a single substrate-binding site for four consecutive condensation steps. *Biochem J.* 2021;**478**:1023–42.
- 51 Li N, Chu X, Wu L, Liu X, Li D. Functional studies of rat hydroxymethylbilane synthase. *Bioorg Chem.* 2008;**36**:241–51.
- 52 Bustad HJ, Kallio JP, Laitaoja M, Toska K, Kursula I, Martinez A, et al. Characterization of porphobilinogen deaminase mutants reveals that arginine-173 is crucial for polypyrrole elongation mechanism. *iScience.* 2021;**24**:102152.
- 53 Bung N, Roy A, Chen B, Das D, Pradhan M, Yasuda M, et al. Human hydroxymethylbilane synthase: molecular dynamics of the pyrrole chain elongation identifies step-specific residues that cause AIP. *Proc Natl Acad Sci USA.* 2018;**115**:E4071–80.
- 54 Jordan PM, Woodcock SC. Mutagenesis of arginine residues in the catalytic cleft of *Escherichia coli* porphobilinogen deaminase that affects dipyrromethane cofactor assembly and tetrapyrrole chain initiation and elongation. *Biochem J.* 1991;**280**(Pt 2):445–9.
- 55 Gill R, Kolstoe SE, Mohammed F, Al D-Bass A, Mosely JE, Sarwar M, et al. Structure of human porphobilinogen deaminase at 2.8 Å: the molecular basis of acute intermittent porphyria. *Biochem J.* 2009;**420**:17–25.
- 56 Lander M, Pitt AR, Alefounder PR, Bardy D, Abell C, Battersby AR. Studies on the mechanism of hydroxymethylbilane synthase concerning the role of arginine residues in substrate binding. *Biochem J.* 1991;**275**(Pt 2):447–52.
- 57 Lenglet H, Schmitt C, Grange T, Manceau H, Karboul N, Bouchet-Crivat F, et al. From a dominant to an oligogenic model of inheritance with environmental modifiers in acute intermittent porphyria. *Hum Mol Genet.* 2018;**27**:1164–73.
- 58 Brownlie PD, Lambert R, Louie GV, Jordan PM, Blundell TL, Warren MJ, et al. The three-dimensional structures of mutants of porphobilinogen deaminase: toward an understanding of the structural basis of acute intermittent porphyria. *Protein Sci.* 1994;**3**:1644–50.
- 59 Roberts A, Gill R, Hussey RJ, Mikolajek H, Erskine PT, Cooper JB, et al. Insights into the mechanism of pyrrole polymerization catalysed by porphobilinogen deaminase: high-resolution X-ray studies of the *Arabidopsis thaliana* enzyme. *Acta Crystallogr D Biol Crystallogr.* 2013;**69**:471–85.
- 60 von Brasch L, Zang C, Haverkamp T, Schlechte H, Heckers H, Petrides PE. Molecular analysis of acute intermittent porphyria: mutation screening in 20 patients in Germany reveals 11 novel mutations. *Blood Cells Mol Dis.* 2004;**32**:309–14.
- 61 Gregor A, Schneider-Yin X, Szlendak U, Wettstein A, Lipniacka A, Rufenacht UB, et al. Molecular study of the hydroxymethylbilane synthase gene (HMBS) among Polish patients with acute intermittent porphyria. *Hum Mutat.* 2002;**19**:310.
- 62 Whatley SD, Woolf JR, Elder GH. Comparison of complementary and genomic DNA sequencing for the detection of mutations in the HMBS gene in British patients with acute intermittent porphyria: identification of 25 novel mutations. *Hum Genet.* 1999;**104**:505–10.
- 63 Cooper DN, Youssoufian H. The CpG dinucleotide and human genetic disease. *Hum Genet.* 1988;**78**:151–5.

## Supporting information

Additional supporting information may be found online in the Supporting Information section at the end of the article.

**Fig. S1.** High-resolution mass spectra of HMBS-variant p.R26H. (A) p.R26H measured at denaturing conditions with 1  $\mu$ M protein. Numbers denote different protein ion-charge states as  $[M+nH]^{n+}$ . The high charges and wide charge state distribution indicate that the protein is fully unfolded. Uroporphyrinogen is also detected in denaturing conditions. (B) p.R26H in native-like conditions at 5  $\mu$ M concentration. Low charges and narrow charge state distribution show that the protein is folded, and the mutation does not cause an unfolding of the enzyme.

**Fig. S2.** Mass spectra of wt-HMBS and p.R26H with PBG. (A) Purified wt-HMBS enzyme showing a mixture of the intermediates  $E_{apo}$ ,  $E_{holo}$ , ES, ES<sub>2</sub> and ES<sub>3</sub>. (B) wt-HMBS with 10 $\times$  PBG, showing the rapid

formation (~1 min) of the ES<sub>4</sub> intermediate. (C) Incubation of the wt-HMBS-PBG mixture for 60 min shows the re-appearance of the previous intermediates. (D) p.R26H incubated with 10× PBG for 24 h shows ES<sub>2</sub> form, indicating a lack of activity. Additional peaks correspond to non-covalent binding of acetate ions. All samples were measured in native-like conditions in 20 mM NH<sub>4</sub>OAc (pH 6.8) at 5 μM enzyme and 50 μM PBG.

**Fig. S3.** The catalytic activity of wt-HMBS and p.R26H as a function of substrate (PBG) concentration. Wt-HMBS and p.R26H measured at standard

conditions with 2 μg protein and varying PBG concentrations (0–2000 μM) for a reaction time of 4 min at 37 °C. The specific activity of HMBS was defined as nmol of uroporphyrinogen I/h per mg of enzyme, under the given assay conditions. The data were fitted to Michaelis–Menten kinetics.

**Table S1.** Prediction of secondary structure content. The secondary structure content based on far-UV CD spectrum recorded at 190–250 nm was estimated in percentage using the DichroWeb software. Multiple unpaired t-test showed no significant difference between wt-HMBS and p.R26H.